

# A Theoretical Performance Assessment Tool for Myocardial Elastography

E. E. Konofagou, Associate Member, IEEE, W. N. Lee and C. M. Ingrassia

**Abstract**— The main purpose of this paper is to develop a theoretical tool in order to fundamentally characterize the performance of Myocardial Elastography and identify the optimal parameters to be used for the more reliable detection of ischemia or infarction. A complete representation of the left-ventricular function throughout an entire cardiac cycle was previously demonstrated through the use of a 3D finite-element analysis (FEA) model. This FEA model together with an ultrasound image formation model is used here in order to test the performance of 2D Myocardial Elastography at distinct phases of the cardiac cycle and at different states of myocardium, i.e., normal and ischemic, based on in vivo canine data. A previously developed 3D finite-element analysis (FEA) model of a normal canine left ventricle with 80 nodes and 40 elements was used to simulate all main phases of the cardiac cycle. The axial and lateral displacements within multiple image (x-y) planes across the left-ventricular volume were iteratively calculated and corrected to reduce the decorrelation noise. Given the excellent agreement between the FEA solution and the elastographic strains measured in 2D over an entire simulated cardiac cycle, Myocardial Elastography proves to be a reliable technique for the accurate assessment of the myocardial deformation in 2D at distinct phases of the cardiac cycle as well as detection of the ischemic region. Preliminary in vivo results of a standard short-axis view in a canine myocardium are shown validating the performance assessment using the proposed model.

## I. INTRODUCTION

Detection of cardiac dysfunction through assessment of the mechanical properties of the heart, and more specifically, the left-ventricular muscle, has been a long-term goal in diagnostic cardiology. This is because both ischemia [1], i.e., the reduced oxygenation of the muscle necessary for its contraction, and infarction, i.e., the complete loss of blood supply inducing myocyte death, alter the mechanical properties and contractility of the myocardium. Acute myocardial infarction caused by partial or total blockage of one or more coronary arteries can cause complex structural alterations of the left-ventricular muscle [2]. These alterations may lead to collagen synthesis and scar formation, which can cause the myocardium to irreversibly

change its mechanical properties. The most comprehensive study on experimental measurement of the stiffness of an acutely infarcted muscle with age was reported by [2]. Gupta et al. [2], in vitro mechanical testing, i.e., biaxial stretching, of an ovine muscle mass corresponding to various times lapsing (0 hrs – 6 weeks) after the induced infarction showed that the stiffness of the infarcted region increased within the first 4 hours, continued to rise by up to 20 times, peaking 1-2 weeks following the infarct and decreasing 4 weeks later (down to 1-10 times the non-infarcted value). The non-infarcted, or remote, myocardium was shown to follow a similar time course but to a much lesser extent. Some of the causes of these mechanical changes have also been reported. Within the first week, deposition of immature collagen as well as increases in fibroblast formation and resorption of necrotic cells occur. By the second week, total loss of normal collagen matrix occurs, followed by abnormal replacement with mature collagen while over time necrotic tissue continues to be resorbed and replaced with scar tissue and some viable muscle cells; hence, the partial decrease of the stiffness after six weeks [2]. The aforementioned complex cellular and histochemical changes directly dictate the mechanical changes of the myocardium. The fact that the mechanical changes induced by the infarct occur right at the onset, and peak two weeks after, indicate the potential for a mechanically-based imaging technique, such as Myocardial Elastography [3], to detect the infarct extent early; employing the same 2D or 3D echocardiographic views as used routinely but possibly detecting it well before a physician can see it.

## II. METHODS AND RESULTS

### 1. Development of a simulated 3D ventricular model

An example of 3D strain estimation under a controlled, externally applied compression was previously shown [4,5]. In the case of the heart, and most notably, the left ventricle, the chamber of the heart most affected by cardiovascular disease, 3D deformation can result from forces that are generated by the myocardium itself. Therefore, the tissue under deformation can no longer be modeled as a passively deformed body. Instead, the cardiac muscle is typically modeled as actively deforming tissue in addition to external stresses, e.g., from blood flow into the ventricular cavity. Therefore, the 3D strain ( $\epsilon_{ij}$ ) will be associated with both passive ( $\sigma_{kl}$ ) and active ( $T_{kl}$ ) stresses through the elasticity

Manuscript received May 2, 2005. This work was supported in part by the American Heart Association under Grant 0435444AT.

E. E. Konofagou is with the departments of biomedical engineering and radiology of Columbia University, New York, NY 10032, USA (212-342-0863; fax: 212-342-5773; e-mail: ek2191@columbia.edu).

W. N. Lee and C.M. Ingrassia are with the department of biomedical engineering of Columbia University, New York, NY 10023, USA (e-mail: w2134@columbia.edu and cmi2001@columbia.edu, respectively).

( $E_{kl}^{ij}$ ) of the myocardium according to a modified version of the Hooke's Law constitutive equation:

$$T_{ij}(t) + \sigma_{ij}(t) = E_{kl}^{ij} \cdot \varepsilon_{kl}(t), \quad (1)$$

where  $k, l, i, j$  are indices that indicate the level of anisotropy, compressibility, etc., and  $t$  denotes time.  $T_{ij}(t)$  denotes the active stress generated by the myocardium and is closely associated to the property of the myocardium to induce a contraction, i.e., the property of contractility.

## 2. Finite-element analysis (FEA) model of left-ventricular mechanics [2,6]

An axisymmetric model has been validated and improved upon by several investigators as the most accurate biomechanical model of the left ventricular mechanics [2,6]. In this model, the left-ventricular muscle is defined in prolate spheroidal coordinates [2] and passively deforming during diastole and actively contracting during systole. The model is a 14-element, trilinear and transversely orthotropic with respect to the muscle fiber axis [2]. The principal axes of the left ventricle are defined in the radial, circumferential and longitudinal directions and the principal strain components are also calculated given that coordinate system. Both these assumptions allow for the reduction in computational complexity of the model without jeopardizing the accuracy of the model when compared to canine heart measurements [2].

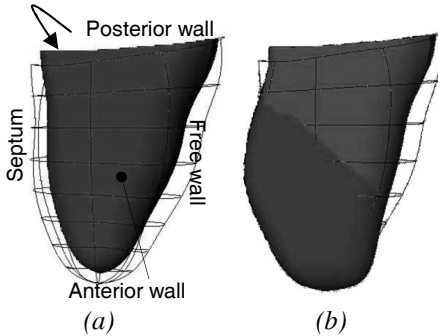


Figure 1: a) Normal left-ventricular representation (i.e., all elements are assigned the same moduli) and b) ischemic left-ventricular representation (i.e., dark elements are assigned a different modulus to denote ischemia/infarct) denoting the areas where the infarct is most likely to occur. [Images (a) and (b) courtesy of the Cardiovascular Biomechanics Group, Columbia University].

The passive material properties of the ventricular wall are defined in terms of a strain energy potential  $W$  that changes exponentially with the strain components  $\varepsilon_{kl}$ , given by

$$W = \frac{C}{2}(e^Q - 1) \quad \text{and} \quad \varepsilon_{kl} = \frac{1}{2} \left( \frac{\partial X^\alpha}{\partial V^k} \frac{\partial X^\alpha}{\partial V^l} - \delta_{kl} \right),$$

where  $C$  denotes the compliance (equal to 0.876 kPa, which matches epicardial strains in intact canine heart preparations [6]),  $Q$  is a parameter that depends on all 3D normal and shear strain

components, i.e.,  $\varepsilon_{kl}$ , for a transversely isotropic model,  $X^\alpha$  denotes the deformed rectangular Cartesian coordinates,  $V^k$  are the fiber coordinates and  $\delta_{kl}$  is the Kronecker delta function. Systolic contraction is modeled through the definition of the stress tensor as the sum of the passive three dimensional stress derived from the aforementioned strain energy function and an active component  $T_{ij}(t, C_{Ca}, l)$  changing with intracellular calcium concentration ( $C_{Ca}$ ) and sarcomere length ( $l$ ). This model is also referred to as a 'time-varying elastance model' and has been suitable for modeling the mechanics of ventricular contraction at end-systole [2]. To simulate a cardiac cycle, the model is passively loaded by an end-diastolic pressure of 0.63 kPa and actively contracting against an end-systolic pressure of 14 kPa. These values have previously been obtained experimentally. Finally, also based on experimental findings on canine isolated hearts using previously described invasive techniques, the model can accurately represent both normal and pathological cases of myocardial deformation of the left-ventricle (Fig. 1).

## 3. Image formation and elastographic estimation from the FEA model

In order to test the feasibility of elastography to reliably depict the strains calculated from the finite-element model described above, the image formation model used in elastography [4-5] was employed. The nodes and elements from the FEA model were considered and short-axis echocardiograms were generated assuming a two-dimensional point-spread function at 5 MHz, 60% fractional bandwidth and 128 RF signals. The scatterers were assumed to be normally distributed at 40 scatterers/wavelength in order to simulate 'full speckle' conditions in the myocardium. The cavity was assumed to have null scattering. This was repeated for each transverse slice of the prolate spheroid of Fig. 1(a) to obtain a 3D echocardiogram (Fig. 2(a)). Each 2D B-mode image is the size of 80mm-by-80mm. Cross-correlation techniques similar those described in [4] were employed on the ultrasonic RF images using a window size equal to 3 mm and an overlap of 80% in order to compute the displacement. The elastogram is obtained by a least-squares strain estimator [7] with a kernel of 5mm. The displacement images and elastograms (or, strain images) at the beginning of diastole, or, the filling phase are shown at good comparison to those computed using the FEA model (Fig. 2(b-e)). The initial model contains eight nodes for each 2D short-axis slice, so the bicubic Hermite interpolation [8] is applied to get the refined mesh. The displacement vectors in the refined model between the unloaded and inflated configurations are shown in Fig. 2(b), where the inner and outer contours indicate the motion of endocardium and

epicardium, respectively. The finite element models of the left ventricle are based on prolate coordinate while the ultrasonic image formation model (Fig. 2(a)) is based on Cartesian coordinates. Thus, the prolate coordinates  $(\lambda, \mu, \theta)$  were converted into Cartesian coordinates  $(x, y, z)$ , where  $x$ ,  $y$ , and  $z$  are the lateral, axial and elevational directions, respectively of the ultrasound plane.

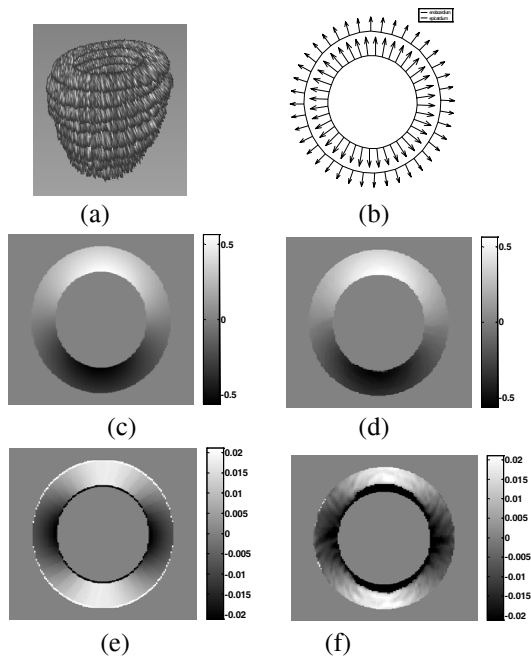


**Figure 2:** Short-axis simulation results at a single phase (close to end-diastole) from the CBG model: a) 3D simulated echocardiogram of the model shown in Fig. 1(a), b) endocardial (inner) and epicardial (outer) x-y displacement; c) computed FEA and d) elastographic axial displacement (mm) and e) computed FEA and f) elastographic axial strain (not in %). Note that the reference in this case is the ultrasound beam and not the fiber orientation.

There are 80 nodes and 40 elements for each 2D short-axis slice of the refined left ventricular model (Fig. 2 (b)). Each node has its own displacement vector. The displacement is calculated by subtracting the coordinates of the same node number of two different models. With the known displacement vectors of each node, the four-point two-dimensional approximation was implemented in order to obtain all the displacement vectors in the myocardium. The axial displacement images and elastograms calculated from the FEA model and estimated using elastographic techniques are shown in Fig. 2(c-d) and (e-f), respectively. In Fig. 3, the lateral displacement (Fig. 3(a-b)) and strain (Fig. 3(c-d)) results are shown in a similar fashion. An iterative correction technique can be used in order to estimate the lateral motion and deformation following full removal of the axial decorrelation [5]. Figure 3 shows the ideal outcome of the recorrelation technique, i.e., when the decorrelation noise due to the axial motion has fully been removed (Figs. 3(b) and 3(d)).

The FEA results shown in Figs. 2 and 3 correspond to the

late passive filling phase of the cardiac cycle (where the left-ventricular pressure changes from 3 kPa to 4 kPa) and the estimation results based on our technique show good agreement with the FEA solutions. A full, simulated cardiac cycle was composed of three phases: *passive filling*, *time-varying elastance*, and *constant elastance*. The passive filling phase involves passive dilation of the model from stress-free condition, which is at zero pressure and a volume of 36 ml. The time-varying elastance phases are obtained at each step of the activation. At maximum elastance, i.e., when the intracellular  $\text{Ca}^{++}$  concentration is at its peak, the model is inflated up to 20 kPa corresponding to end systole (ES). During the constant elastance phase the displacements are computed at maximum elastance by reducing the pressure down to zero kPa at 33.4 ml.

Figure 4 shows the mean axial strain within two selected regions during the entire simulated cardiac cycle as indicated in Figs. 4 (a) and (b). The mean axial strains of the FEA solution and the elastographic measurements are at excellent agreement, highlighting thus the good performance of Myocardial Elastography throughout the entire cardiac cycle. In addition, the change of the axial strain at different phases accurately quantifies the amount of contraction or tension of the myocardium. Similar results were obtained in the case of the lateral estimation.

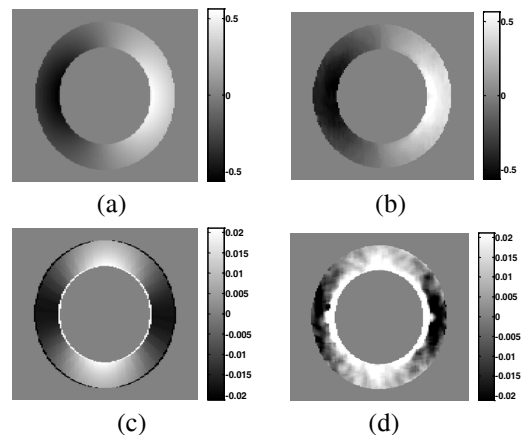


**Figure 3:** Short-axis simulation results at a single phase (close to end-diastole) with zero axial displacement: a) computed FEA and b) elastographic lateral displacement (mm) and c) computed FEA and d) elastographic lateral strain (not in %). Note that the reference in this case is the ultrasound beam and not the fiber orientation.

#### 4. In vivo validation

2D echocardiographic RF data using a portable, laptop scanner (Terason 2000, Teratech, Inc) and a 3 MHz phased array were acquired continuously during a 2-min induction of acute myocardial infarction through ligation of the left-ascending, distal (LAD) coronary artery of an open-chested dog (respiration was also interrupted). Sequences of ultrasound RF images were acquired at 54 frames/s (128 RF lines, sampling frequency: 10MHz).

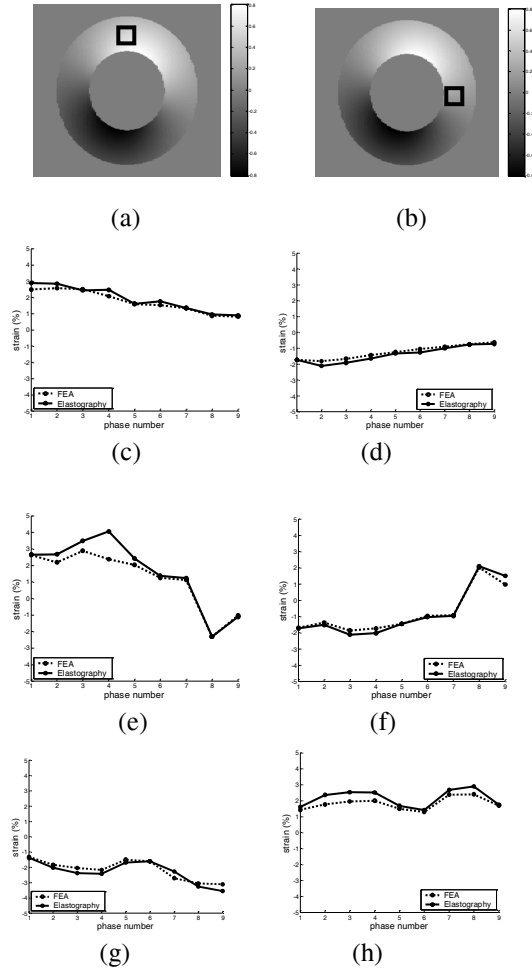


**Figure 4:** The axial strain variations at different phases of the full cardiac cycle as calculated in FEA (dashed curves) and estimated in elastography (solid curves): a) and b) the mean strains are calculated in the regions as shown by the rectangles on an FEA displacement image; c) and d) mean axial strain (%) during the passive filling phases (as indicated in sequence) in the regions shown in a) and b), respectively; e) and f) mean axial strain (%) during the time-varying elastance phases; g) and h) mean axial strain (%) during the constant elastance phases.

Axial displacements are estimated from two consecutive RF frames, using a 1D cross-correlation algorithm (Size of the correlation windows: 6 mm; overlapping: 90%). In this algorithm, time-shifts between two consecutive backscattered signals are determined by the cross-correlation of small sliding windows over the entire 2D ultrasound image. Finally, the strain distribution is computed by differentiating the displacement map along the axial direction. For the numerical differentiation a least-squares regression method was used. The results show how elastograms and elastocardiograms (i.e., the overlaid echocardiogram and elastogram image, Fig. 5) can be used to localize the region of the muscle undergoing ischemia (denoted by low strain (close to zero) between 3 o'clock and 6 o'clock, which coincides with the LAD ligated region).

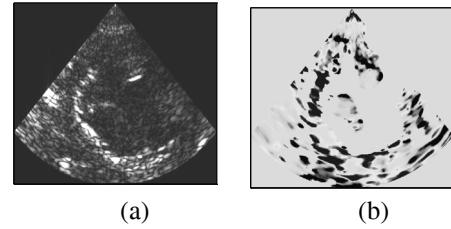


**Figure 5:** Example of a) Short-axis echocardiogram, b) axial elastogram at the beginning of the LAD ligation at end-diastole. The strain ranges from +1% (compressive strain) to -1% (tensile strain).

### III. CONCLUSION

A theoretical model was developed that takes into account the 2D motion of the left-ventricular muscle throughout an entire, simulated cardiac cycle with three distinct phases. The 2D normal strain components were estimated throughout the full cycle and compared to the “ideal” cases, i.e., the solutions of the FEA model. The model prepared is a useful tool for the prediction of the elastographic performance prior to its in vivo application. Ongoing investigations include in vivo validation of the 2D and 3D strain estimation and the development of an ischemic left-ventricular model.

### IV. ACKNOWLEDGMENTS

This study was supported by a Scientist Development grant from the American Heart Association. The authors also wish to thank Kevin Costa and Jeff Holmes for guidance with the FEA model calculations and Mathieu Pernot for the in vivo data processing.

### V. REFERENCES

- [1] Haga J.H., Beaudoin A.J., White J.G. and Strony J., *Ann Biomed. Eng.* 26, 268-277, 1998.
- [2] Guccione J.M., Costa K.D. and McCulloch A.D., *J. Biomechanics* 28, 1167-1117, 1995.
- [3] Konofagou E.E., D’hooge J. and Ophir J., 475-482, 2002.
- [4] Konofagou E.E., Kallel F. and Ophir J., *IEEE-UFFC Proc Symp.*, 1745-1748, 1998.
- [5] Konofagou E.E. and Ophir, J., *Ultras Med Biol* 24, 1183-1199, 1998.
- [6] Guccione J. M., McCulloch A. D. and Waldman L. K., *ASME J. Biomech. Eng* 113, 42-55, 1991.
- [7] Kallel, F. and Ophir, J., *Ultrasonic Imaging* 19, 195-208, 1997.
- [8] Hashima, A.R., Young, A.A., McCulloch, A.D. and Waldman, L.K., *J. Biomechanics*, 26, 19-35, 1993.